Effect of ball milling strategy (milling device for scaling-up) on the hydrolysis performance of Mg alloy waste

Serge Al Bacha, Santiago A. Pighin, Guillermina Urretavizcaya, Mirvat Zakhour, Michel Nakhl, Facundo J. Castro, Jean-Louis Bobet

Effect of ball milling strategy (milling device for scaling-up) on the hydrolysis performance of Mg alloy waste

S. Al Bacha[a,b], S.A. Pighin[c,d], G. Urretavizcaya[c,e], M. Zakhour[a], M. Nakhl[a], F.J. Castro[c,e], J.-L. Bobet[b]*.

[a] LCPM/PR2N (EDST), Lebanese University, Faculty of Sciences II, 90656 Jdeidet El Metn, Lebanon.

[b] University of Bordeaux, CNRS, Bordeaux INP, ICMCB, UMR 5026, F-33600 Pessac, France.

[c] CNEA, CONICET, Centro Atómico Bariloche, S.C. de Bariloche, Río Negro, Argentina.

[d] Universidad Nacional del Comahue, Centro Regional Universitario Bariloche, S.C. de Bariloche, Río Negro, Argentina.

[e] Universidad Nacional de Cuyo, Instituto Balseiro, S.C. Bariloche, Río Negro, Argentina.

Abstract

Ball milling strategy is of prime importance on the hydrolysis performance of Mg alloy waste. The effect of milling device (*e.g.* Fritsch Pulverisette 6 (P6) and Australian Uni-Ball-II (UB)), milling atmosphere (H_2 and Ar), milling time, nature of the additives graphite and $AlCl_3$ and synergetic effect by chronological or simultaneous addition were examined. An equivalence between both mills was established and it was shown that the process with the UB is 10 times longer than that with the P6 to acquire a similar material. Mg alloy milled without additives in the P6 under Ar for 10h improves the hydrolysis performance. Using a single additive, the best hydrolysis performances are obtained with graphite (yield of 95% of total capacity reached in 5 minutes) due to the formation of a protective graphite layer. By incorporating both additives sequentially, the best material, from the hydrogen production point of view, was Mg alloy milled with G for 2h and then with $AlCl_3$ for 2 extra hours (full hydrolysis in 5 minutes). Mg alloy milled with the P6 were compared to those milled with the UB. Mg alloy milled with graphite or with sequential addition of G and $AlCl_3$ under Ar generated more than 90% of their total capacity. Our results confirm that laboratory- milling strategy can be scaled-up to industrial scale.

Keywords: Mg alloy waste; ball milling; hydrolysis reaction; hydrogen; milling atmosphere; synergetic effect.

* Corresponding author: jean-louis.bobet@cnrs.fr, (J.-L. Bobet).

1. Introduction

Ball milling is a simple and effective processing technique that induces structural, morphological and microstructural modification of materials by energetic impacts (balls to balls and balls to wall). Moreover, this technique can induce chemical reactions that do not normally occur at room temperature [1]. For this reason, ball milling in its various forms (*e.g.* mechanical alloying, reactive ball milling, etc.) is very commonly used in many areas of materials science and green chemistry, and recently in most experiments on hydrogen storage/production from Mg-based materials [1-7]. Based on the movement of the balls and the vial, various type of milling devices can be distinguished such as planetary, vibrational, rotational, magnetic and attrition mills [8, 9]. The planetary ball mill is one of the most popular and most effective at the same time [8].

The properties of the milled material depend on many parameters such as the type of mill, milling speed or frequency, milling time, milling atmosphere, ball-to-powder weight ratio, etc. [9]. During the milling process, significant heat is locally generated and this can affect the process [9]. Hence, rests are often included during high energy milling processes to avoid excessive heating of the sample, so that various milling strategies have been described in recent years.

Grosjean *et al.* [10] were the first to report the beneficial effect of milling on the improvement of corrosion of Mg and therefore on its hydrolysis. Particles size reduction promotes the dissolution of the passivation layer of $MgO/Mg(OH)_2$ [3, 4, 11, 12] resulting in an improvement of the hydrolysis performance of Mg (*e.g.* by increasing the number of hydrolysis initiator sites). From the last two decades, several studies have shown that ball milling of Mg-based materials under Ar with additives (*e.g.* metals [4, 7, 13-19], salts [2, 11, 16, 17, 20-25], graphite [2, 4, 7, 11], oxides [4, 26], sulphides [27]) improved the hydrolysis performances. It was proven that Mg-based wastes

can be used to generate H_2 by hydrolysis reaction [2, 7, 28-33]. Moreover, ball milling with [7] and without [32] additives has been shown to ameliorate the hydrolysis reaction of Mg-based wastes.

The author's earlier works [2, 11] have stated that the addition of cheap additives such as graphite and $AlCl_3$ during ball milling of $Mg_{17}Al_{12}$ and a Mg alloy was beneficial to their hydrolysis performance. In our previous work, we have studied the effects of reactive ball milling (under H_2) and the singular and synergetic addition of graphite and $AlCl_3$ on the hydrolysis performances of Mg alloy waste [2]. We have shown that increasing the milling time without additive beyond 2h reduces the hydrolysis performance. Adding $AlCl_3$ slightly improves the hydrogen production properties after 2 hours of milling while incorporating graphite (as single additive) moderately reduces the hydrolysis properties. On the other hand, the simultaneous or chronological addition, and the order of incorporation of graphite and $AlCl_3$ strongly affect the microstructural properties of the material, and consequently the hydrogen production performance. Milling under H_2 may form MgH_2 which increases the total hydrogen generation capacity of the material but also decreases the kinetics due to the lower reactivity of MgH_2 compared with Mg [34].

In the present work, we have established an equivalence between 2 milling devices: the "high-energy" Fritsch Pulverisette 6 and the "low-energy" Uni-Ball-II to simulate the transition from the laboratory to the industrial scale. Given the risk of using hydrogen in industrial applications, we compared Mg alloy milled under H_2 and under Ar using both mills. The effects of the ball milling time, the use of additives (graphite and $AlCl_3$) and the synergetic effect of adding both additives in all strategies (*i.e.* ball milling using (i) the Pulverisette 6 under H_2 [2] and Ar and (ii) the Uni-Ball-II under Ar were discussed. The results presented will allow us to establish the best strategy for activating Mg alloy waste in order to produce hydrogen by the hydrolysis reaction. It will also give us some trends to upscale the process.

2. Experimental details

Waste of Mg-based alloy from the machining of sacrificial anodes for water heaters mixed with some Al scraps (as provided by Roberto Cordes S.A., Argentina) was cleaned with acetone following the procedure reported in our previous study [2]. In this reference the material was reported as "Mg alloy", but subsequent analysis has shown that the material was a real manufacturing waste composed of scraps of AZ31 mixed with some Al scraps in a proportion closer to that of AZ91. The global amount of Al and Zn in the material was estimated by Inductively Coupled Argon Plasma (using a Varian 720ES ICP-OES spectrometer) elemental analysis is detailed in Table 1.

Table 1: Nominal composition of Mg alloy magnesium waste in wt.%

Element	Al	Zn	Mg
Content (wt.%)	8.1	0.9	Bal.

Mg alloy milling was performed under 5 bar of H_2 or Ar at room temperature in a (i) "low-energy" (maximum rotation speed of 200 rpm) milling device Uni-Ball-Mill II, from Australian Scientific Instruments, with a double magnet in the bottom vertical position (subsequently named UB) and (ii) "high-energy" (maximum rotation speed of 600 rpm) planetary mono mill Fritsch Pulversitte 6 (subsequently named P6). The ball-to-powder mass ratio was fixed to 40:1 in both cases. The rotational speed in the UB was fixed to 185 rpm without a pause (continuous milling). The milling with the P6 was performed at 400 rpm with the sequence of 10 minutes of milling followed by 20 minutes of rest [2]. Graphite powder G (99%, Aldrich) and anhydrous aluminum chloride powder $AlCl_3$ (98%, Aldrich) were used as additives.

To minimize the air exposure, the materials were stored in argon-filled glove box. Nevertheless, before any hydrolysis tests, it was mandatory to expose the sample to air but we succeed to limit it to a maximum of 7 minutes.

Hydrolysis tests tests (Room temperature and atmospheric pressure, 20 mg of sample with 100ml of salted water) were performed following the same procedure described in references [2, 34]. 10 ml of a 0.5M HCl solution were added to the reactor after 60 minutes of starting of the hydrolysis test to complete the reaction. The volume of H_2 generated after the addition of HCl corresponds to the theoretical volume calculated by considering the hydrolysis of Mg, MgH_2 and Al. The amount of each phase was estimated from XRD refinements.

Mg alloy milled materials were analyzed by X-ray diffraction (Bruker Advance D8 diffractometer with Cu Kα radiation), laser granulometry in ethanol (Malvern Mastersizer hydro 2000® analyzer) and scanning electron microscopy (SEM-FIB Zeiss Crossbeam 340 coupled to an EDS detector). The crystalline phases identification was done using the ICDD database and quantification was estimated by Rietveld refinement using TOPAS [35]. The crystallites size (τ) was calculated according to the weighted Scherrer formula. The amount of Al incorporated into the Mg matrix (x_{Al}, occupancy) was estimated from the relationship between cell parameter and solubility established by ref [36]. Particles size data are expressed as number distribution (d_{90}). Note that d_{90} corresponds to the maximum diameter of 90% of the particles.

Before any analysis, the obtained powder was passed through a sieve of 200 µm, unless no powder was contained in the product of ball milling.

Throughout this work, the materials will be named as follows:

- Mg alloy mh: Mg alloy milled for m hours,
- Mg alloy + X mh: Mg alloy milled with 5 wt.% of X for m hours,
- Mg alloy + (X + Y) mh: Mg alloy milled with 5 wt.% of X and 5 wt.% of Y for m hours and
- Mg alloy + X mh + Y nh: Mg alloy milled with 5 wt.% of X for m hours followed by a milling with 5 wt.% of Y for n hours, (X,Y = $AlCl_3$, G).

3. Results and discussion

3.1.Equivalence between P6 and UB mills

Industrial mills are much larger than laboratory mills such as P6. On the other hand, high energy laboratory mills allow to reduce milling time [9, 37]. To establish an equivalence between both milling devices, the hydriding of Mg has been selected as an easy indicator of the milling efficiency since it depends on the morphology and the structure of the milled material. Therefore, Mg alloy was milled under H_2 using both mills (*i.e.* P6 and UB) and the amount of MgH_2 formed was determined.

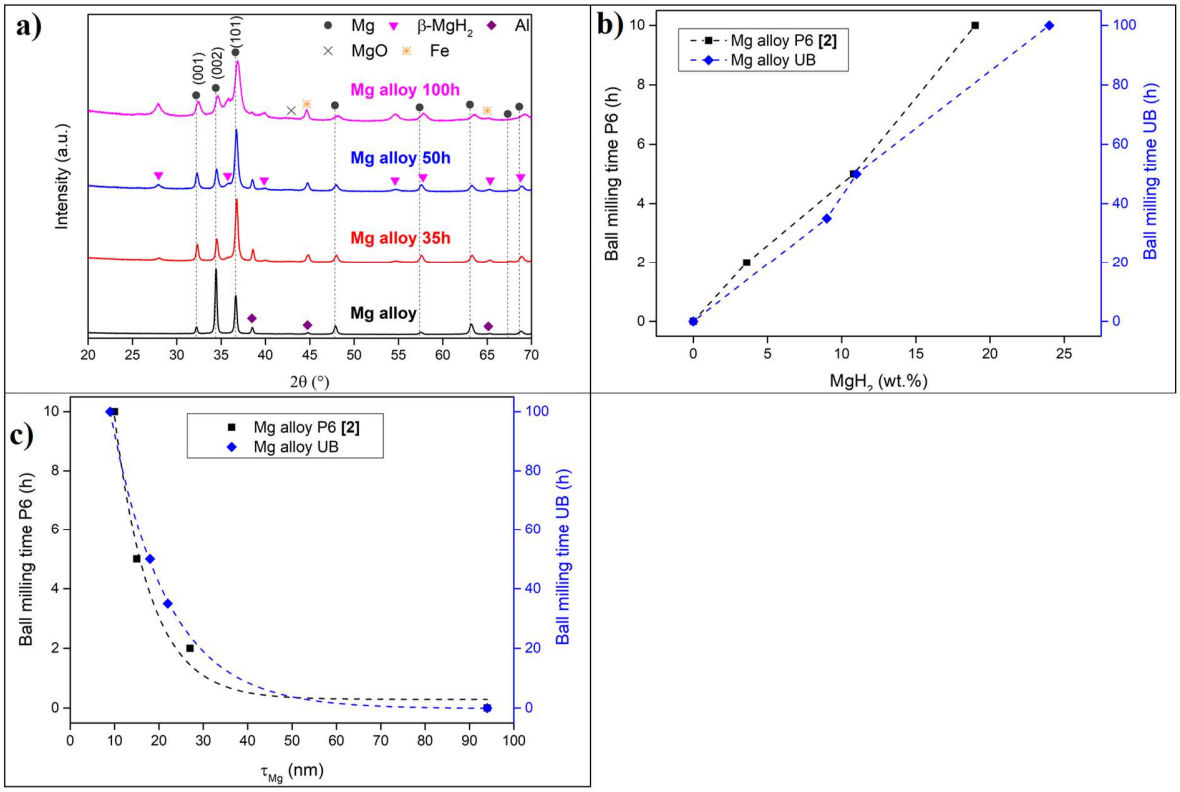

Figure 1: a) XRD patterns of Mg alloy, Mg alloy milled with the UB under H_2 for 35h, 50h and 100h; variation of b) MgH_2 amount and c) Mg crystallites size (τ_{Mg}) in Mg alloy milled without additives under H_2 with the P6 [2] and with the UB.

Figure 1.a shows that ball milling with the UB mill (for 35h, 50h and 100h) modifies the structure of the alloy as observed with the P6 mill [2]. During prolonged milling, large energy is

accumulated into the material, dislocations occur in all directions and therefore Mg preferential orientation along the c axis (*i.e.* maximum intensity for the (002) plane of Mg) disappears [2, 7, 10]. Moreover, milling for longer duration (*i.e.* 100h) increases Fe contamination from the milling jar and balls. As observed during ball milling of Mg alloy under H_2 in the P6 [2], the more Mg peaks are shifted towards higher 2θ angles, the more Al atoms are inserted in the Mg matrix (*i.e.* the occupancy of Al in Mg (x_{Al}) increases from 2 at.% after 35h of milling to 5.6 at.% after 100h of milling). As milling proceeds, Mg peaks width broadens as a consequence of crystallites size reduction. Ball milling of Mg alloy activates its Mg matrix (*i.e.* crystallites and particles size decrease, *Cf* Table 2) which reacts with the hydrogen of the milling chamber to form β-MgH_2. The amount of MgH_2 increases from 9 wt.% to 24 wt.% by prolonging the milling from 35h to 100h (Table 2). From Figure 1.b and Table 2, it should be noted that the content of MgH_2 in Mg alloy milled with the P6 for 5h and Mg alloy milled with the UB for 50h is almost similar. The one order of magnitude between the milling time with P6 and UB can also be highlighted for the evolution of the Mg crystallites size as seen from Figure 1.c.

Table 2: Quantification of Mg, β-MgH_2 and γ –MgH_2, Al atoms occupancy in Mg matrix (x_{Al}), Mg crystallites size (τ_{Mg}) and particle size d_{90} of MG ALLOY milled under H_2 without additives in the P6 [2] and in the UB mill.

Mill device	**Sample**	**Rietveld refinement from XRD measurements**					**Particle size d_{90} (µm)**
		Mg*	β-MgH_2*	γ – MgH_2 *	x_{Al} in Mg (at.%)	τ_{Mg} (nm)	
	Mg alloy	87	0	0	2.2	94	+
P6 [2]	Mg alloy 2h	89	3	0.6	1.9	27	32
	Mg alloy 5h	82	10	0.8	3.3	15	13
	Mg alloy 10h	77	17	2	6.9	10	11
UB	Mg alloy 35h	79	9	0	2	22	18
	Mg alloy 50h	78	11	0	2.4	18	12
	Mg alloy 100h	69	24	0	5.6	9	7

* values are given in wt.%.
+ the material is not a powder but flakes.

In term of milling energy, many parameters need to be taken into account (*e.g.* rotational speed, size of milling vial, ball-to-powder mass ratio, etc.). Therefore, we can conclude that roughly 1 hour of milling with the P6 is equivalent to 10 hours of milling with the UB.

3.2.Ball milling with the P6 under Ar

Ball milling Mg-based materials under H_2 leads to the formation of MgH_2 which (i) increases the total capacity of hydrogen generation of the milled material but also (ii) decreases the reactivity as MgH_2 is less reactive (in term of hydrolysis performance) than Mg [4, 34].

Hydrogen is a hazard gas with low ignition energy of 0.02 mJ (which is at least 5 times lower than that of other gases such as benzene or butane, high range of flammability and explosion, etc.) and has also a severe impact on materials (*e.g.* hydrogen embrittlement of steel) [38]. Milling under H_2 can, therefore, lead to serious risks (i) on the milling tools (*e.g.* milling chamber and milling balls) or (ii) in the case of a leak in the system. Then, we investigated the effect of ball milling under inert atmosphere such as Ar in the absence and in the presence of 5 wt.% of additives (*i.e.* graphite and $AlCl_3$), and the synergistic effect by chronological or simultaneous addition of both additives.

3.2.1. Effect of ball milling time

Milling Mg alloy without additives for 2, 5 and 10h accumulates energy in the powder which causes the disappearance of the preferential orientation of Mg along the c-axis [38] (Figure 2.a). As mentioned before [2], the shift of Mg XRD peaks toward higher 2θ angles is due to the insertion of Al atoms into the Mg matrix. Al atoms occupancy in Mg matrix (x_{Al}) increases from 2.2 at.% to 7.2 at.% after 10h of milling (Table 3). The peaks broadening is attributed to the reduction in crystallite size (from 27 nm to 10 nm, *Cf* Table 3). Also, at longer milling times, the peak attributed to Fe grows indicating an increased amount of contamination from the milling tools (Figure 2.a).

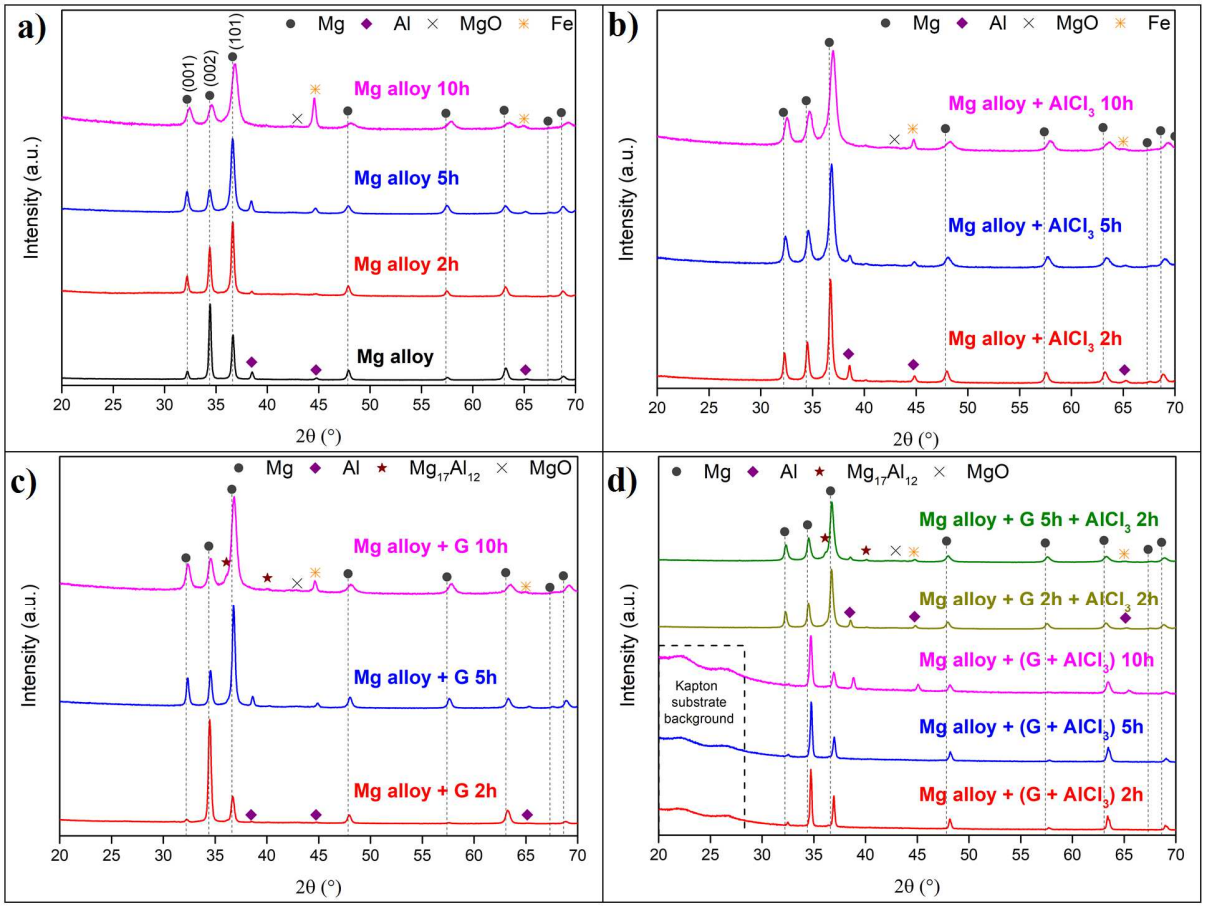

Figure 2: XRD patterns of a) Mg alloy milled without additives, b) Mg alloy milled with $AlCl_3$, c) Mg alloy milled with G and d) Mg alloy milled with G and $AlCl_3$ under Ar with the P6.

From Table 3, it is shown that particle size d_{90} decreases from 54 µm to 19 µm by prolonging milling time from 2h to 10h.

Table 3: Al atoms occupancy in Mg matrix (x_{Al}), Mg crystallites size (τ_{Mg}) and particle size d_{90} of all Mg alloy milled with the P6 mill under Ar atmosphere.

Sample	**Rietveld refinement from XRD measurements**		**Particle size d_{90} (µm)**
	x_{Al} in Mg (at.%)	τ_{Mg} (nm)	
Mg alloy	2.2	94	+
Mg alloy 2h	1.8	27	54
Mg alloy 5h	2.2	17	23
Mg alloy 10h	7.2	10	19
Mg alloy + $AlCl_3$ 2h	1.8	23	14
Mg alloy + $AlCl_3$ 5h	3.2	13	13
Mg alloy + $AlCl_3$ 10h	6.1	10	10
Mg alloy + G 2h	1.7	28	+
Mg alloy + G 5h	1.6	25	21
Mg alloy + G 10h	5.3	12	16
Mg alloy + (G + $AlCl_3$) 2h	1.5	91	+
Mg alloy + (G + $AlCl_3$) 5h	1.4	38	+
Mg alloy + (G + $AlCl_3$) 10h	1.5	29	+
Mg alloy + G 2h + $AlCl_3$ 2h	1.7	23	12
Mg alloy + G 5h + $AlCl_3$ 2h	2.2	17	8

+ the material is not a powder but flakes.

Mg alloy milled without additives under H_2 (Table 2) and Ar (Table 3) gives similar Mg crystallite sizes while milling under H_2 leads to smaller particles. This may be attributed to the formation of the brittle MgH_2 that helps to enhance the decrease of particles size.

Table 4: Hydrogen production by hydrolysis with Mg alloy milled with the P6 mill under Ar atmosphere after 5 minutes and 60 minutes of reaction in 0.6M $MgCl_2$ solution, after 0.5M HCl solution addition considered as being the total hydrogen amount produced) and the calculated yield.

Sample	**H_2 generation in 0.6M $MgCl_2$ after 5 minutes**		**60 minutes**		**H_2 (wt.%) generation in 0.5M HCl****
	H_2 (wt.%)	Yield (%)*	H_2 (wt.%)	Yield (%)*	
Mg alloy	0.03 ± 0.03	0.5	1.1 ± 0.1	17.2	6.7 ± 0.2
Mg alloy 2h	3.2 ± 0.1	40.2	7.5 ± 0.2	94.9	8.0 ± 0.4
Mg alloy 5h	4.1 ± 0.1	53.6	6.0 ± 0.2	78.4	7.6 ± 0.3
Mg alloy 10h	5.8 ± 0.2	81.0	6.5 ± 0.2	89.9	7.2 ± 0.3
Mg alloy + $AlCl_3$ 2h	4.9 ± 0.1	74.0	5.9 ± 0.2	89.1	6.6 ± 0.3
Mg alloy + $AlCl_3$ 5h	3.7 ± 0.1	52.1	4.7 ± 0.1	67.2	7.0 ± 0.3
Mg alloy + $AlCl_3$ 10h	4.3 ± 0.1	56.0	5.1 ± 0.1	67.0	7.6 ± 0.3
Mg alloy + G 2h	4.5 ± 0.1	76.9	5.7 ± 0.2	97.0	5.9 ± 0.3
Mg alloy + G 5h	6.5 ± 0.2	95.3	6.8 ± 0.2	98.8	6.9 ± 0.3
Mg alloy + G 10h	5.7 ± 0.2	77.3	6.8 ± 0.2	92.5	7.3 ± 0.3
Mg alloy + (G + $AlCl_3$) 2h	0.2 ± 0.04	3.6	1.4 ± 0.1	21.9	6.3 ± 0.2
Mg alloy + (G + $AlCl_3$) 5h	0.4 ± 0.04	6.5	1.9 ± 0.1	34.6	5.5 ± 0.2
Mg alloy + (G + $AlCl_3$) 10h	1.0 ± 0.05	15.7	3.7 ± 0.1	55.1	6.6 ± 0.3
Mg alloy + G 2h + $AlCl_3$ 2h	6.0 ± 0.2	97.6	6.1 ± 0.2	99.4	6.1 ± 0.3
Mg alloy + G 5h + $AlCl_3$ 2h	5.9 ± 0.2	90.5	6.0 ± 0.2	92.1	6.5 ± 0.3

* Values are normalized with respect to the total H_2 generated after the addition of 0.5M HCl solution.

** After adding HCl, the hydrolysis reaction is considered complete and the amount of hydrogen produced is considered as the maximum H_2 production.

Unmilled Mg alloy barely reacts in 0.6 M $MgCl_2$ solution with 1.1 wt.% of H_2 generated within 1 hour of hydrolysis reaction (Table 4). According to Table 4, the increase in milling time (*i.e.* 2, 5 and 10h) improved the hydrogen generation in the first 5 minutes (3.2 wt.%, 4.1 wt.% and 5.8 wt.% of H_2 for Mg alloy 2h, 5h and 10h respectively), whereas the hydrogen amount generated after 60 minutes decreases first, and then recuperates a bit, by prolonging milling time. The reduction in particles size (*Cf* Table 3) increases the specific surface area of Mg which reacts rapidly with water (high kinetics during the first minutes) and then, forms the passivation layer $Mg(OH)_2$ [12] which blocks the path of H_2O to react with the Mg core (*i.e.* lower H_2 generation after 60 minutes) [4]. The fact that the surface defects are more efficient than bulk defects [11], the effect of the variation of the crystallites size (*i.e.* bulk defects) on the hydrolysis performances of milled Mg alloy is not taken into consideration.

3.2.2. Singular effect of $AlCl_3$ and G addition

Ball milling Mg alloy with $AlCl_3$ or G under H_2 was proven to be beneficial on the hydrolysis performance [2]. Mg alloy milled with $AlCl_3$ slowed the hydriding of Mg due to the formation of an $AlCl_3$ (partial or total) layer on the surface and 2h of milling was optimal to reach the best hydrolysis performance (92% of its total capacity in 60 minutes). For the graphite, 5h of milling was necessary to improve both Mg hydriding (12 wt.% of MgH_2 formed in Mg alloy + G 5h [2]) and hydrolysis performances (90% of its total capacity in 60 minutes).

The effect of milling with 5 wt.% of each of the 2 additives under Ar was investigated by varying the milling time for 2, 5 and 10h. The preferential orientation along the c-axis of Mg disappears after milling with $AlCl_3$ (Figure 2.b) whereas it persists after 2h of milling with G due to its lubricating effect (Figure 2.c) [4, 7]. $AlCl_3$ and graphite act differently during ball milling. Graphite, by its lubricating effect, does not further improve the milling efficiency while $AlCl_3$ increases its efficiency. In other words, Mg alloy milled with $AlCl_3$ shows smaller Mg crystallites size and particles size compared to Mg alloy milled without additives (*Cf* Table 3). Mg alloy milled with graphite possesses approximately the same τ_{Mg} and d_{90} than Mg alloy milled without additives (*Cf* Table 3).

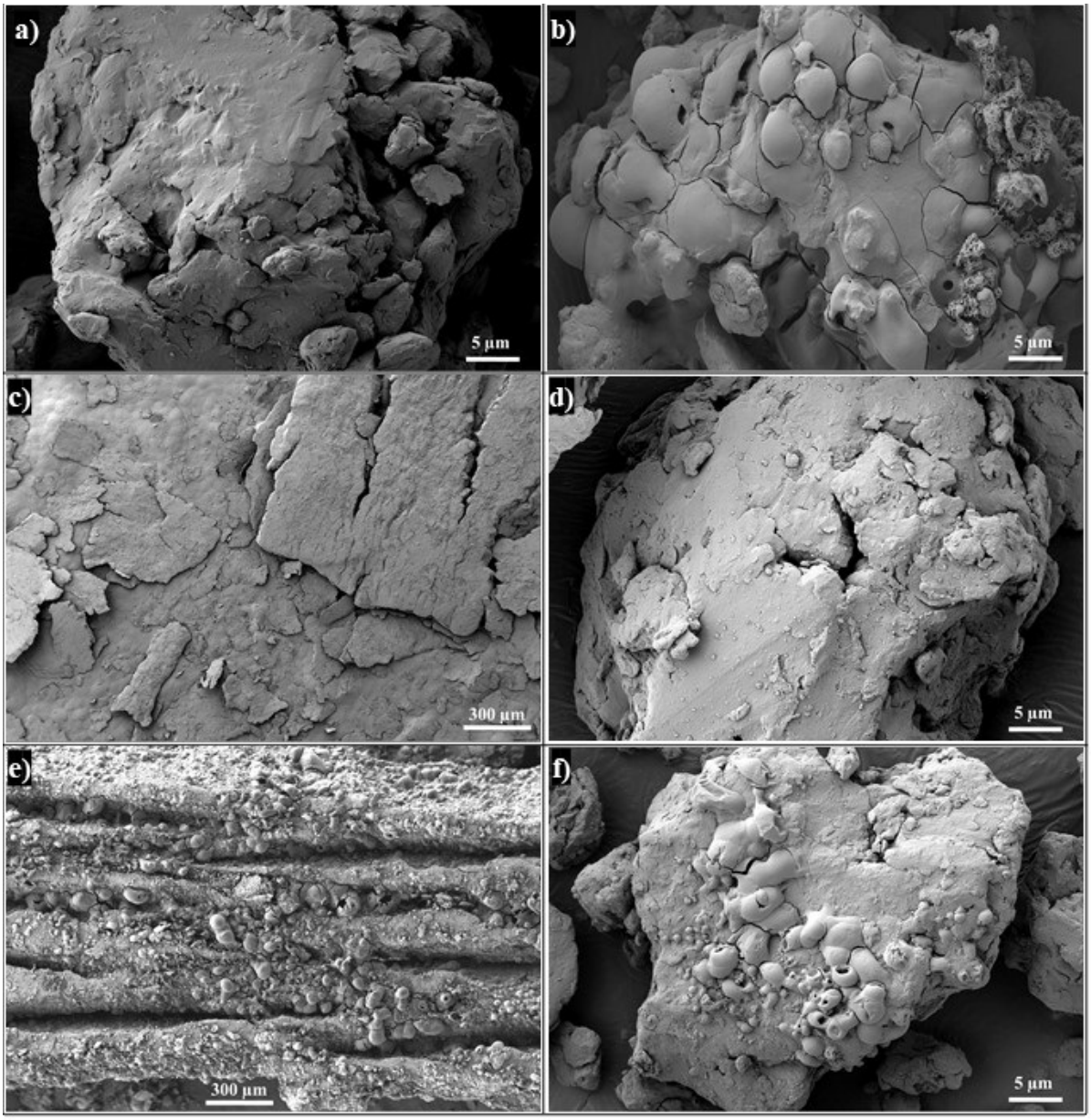

Figure 3: SEM images of a) Mg alloy 10h, b) Mg alloy + $AlCl_3$ 2h, c) Mg alloy + G 2h, d) Mg alloy + G 5h, e) Mg alloy + (G + $AlCl_3$) 10h and f) Mg alloy + G 2h + $AlCl_3$ 2h milled under Ar with the P6.

Milling in the presence of $AlCl_3$ generates surface defects (*i.e.* cracks) and reduces particles size (Figure 3.b) [11, 20, 23, 39] while milling with graphite requires 5 hours to reduce the flakes into powders (Mg alloy + G 2h is not a powder, *Cf* Figure 3.c).

Referring to Table 4, Mg alloy milled 2h with $AlCl_3$ shows better hydrolysis performance than Mg alloy milled without additives (4.9 wt.% of H_2 produced in 5 minutes (*i.e.* yield of 74% of its total capacity) and 5.9 wt.% in 60 minutes (*i.e.* yield of 89% of its total capacity)). The improvement of the hydrolysis kinetics is attributed to (i) the increase of the surface defects which promote pitting corrosion due to Cl^- ions (from $MgCl_2$ solution) and (ii) the exothermic dissolution of $AlCl_3$ during the reaction which generates Lewis acid cation Al^{3+} and Brønsted acid cation H^+ [7, 10, 11] which favors the dissolution of the passive layer of $Mg(OH)_2$ [2, 11, 23]. Nevertheless, as observed for Mg alloy milled with $AlCl_3$ under H_2 [2], milling for more than 2h with $AlCl_3$ decreases the hydrolysis performance due to increased oxidation of the powder and to the homogeneity of the defects distribution in the material after prolonging milling time [40].

Mg alloy + G 5h shows the best hydrolysis performances compared to Mg alloy milled with a single additive, with a generation of 6.5 wt.% H_2 during the first 5 minutes (*i.e.* yield of 95% of its total capacity) and 6.8 wt.% H_2 after 60 minutes (corresponding to a total hydrolysis reaction, *Cf* Table 4). The relative low hydrogen production by hydrolysis with Mg alloy + G 2h (compared to that with Mg alloy + G 5h and 10h) is attributed to the large size of particles (*i.e.* greater than 300 µm, *Cf* Table 3), which reduces the reactive surface area between Mg and H_2O. The low hydrogen production capacity for the latter material (5.9 wt.% H_2, *Cf* Table 4) is explained by the fact that, during ball milling with graphite for 2h, no powder is obtained and graphite is distributed inhomogeneously on the flakes. On the other hand, prolonged milling with graphite (*i.e.* 10h) decrease the hydrolysis performances (Table 4) due to the destabilization of the protective graphite layer on the surface of Mg (formation of graphite agglomerates [7]), and the increased oxidation of the powder and the homogeneity of the defects distribution in the material [40].

However, hydrolysis performances of Mg alloy milled with graphite was better to those of Mg alloy milled without additives and with $AlCl_3$ due to the presence of a graphite layer on the surface which hinders the adhesion of the passive $Mg(OH)_2$ [4, 7].

3.2.3. Synergetic effect of graphite and $AlCl_3$

Up to now, we have shown that milling with $AlCl_3$ for 2h and milling with G for 5h improves the hydrolysis performances of Mg alloy (section 3.2.2). In this context, it is of interest to study the possible synergistic effect by adding 5 wt.% of graphite and $AlCl_3$, either by simultaneous or chronological addition.

Considering the simultaneous addition of G and $AlCl_3$, changing the mill gas (*i.e.* Ar or H_2 [2]) does not reveal significant modification in the structure and morphology of the materials. The crystallographic preferred orientation persists even after 10 hours of ball mill (Figure 2.d) and Al atoms occupancy in Mg matrix does not increase by prolonging milling time (x_{Al} = 1.5 at.%, *Cf* Table 3). Moreover, Mg crystallites size is greater than that of Mg alloy milled for the same duration without additives (91 nm vs. 27 nm for 2h, 38 nm vs. 17 nm for 5h and 29 nm vs. 10 nm for 10h, *Cf* Table 3) and only flakes were obtained with a d_{90} greater than 300 µm (Figure 3.e). It is noticed that increasing ball milling time (*i.e.* 2, 5 and 10h) with both G and $AlCl_3$ simultaneously enhances the hydrolysis performances with a generation of 22%, 35% and 55% of the total hydrogen generation capacity respectively. As observed for Mg alloy + (G + $AlCl_3$) milled under H_2 [2], the simultaneous addition of graphite and $AlCl_3$ somewhat cancels the individual positive effect of each additive, leading to a less efficient milling and then to lower hydrolysis performances (for example, 1 wt.% of H_2 produced in 5 minutes and 3.7 wt.% in 60 minutes for AZ91 + (G + $AlCl_3$) 10h).

When studying the effect of chronological addition of $AlCl_3$ and G, on the basis of our previous results[2], that show that the addition of G after ball milling Mg alloy with $AlCl_3$ for 2h did not reveal a beneficial effect on hydrolysis, such procedure was not taken into consideration in the present work. Therefore, the sequential addition of first G and then $AlCl_3$ was studied, choosing milling times of 2 and 5h for G and of 2h after $AlCl_3$ addition, as this is the optimal milling time with this additive (Section 3.2.2).

The preferential orientation along the c-axis in Mg alloy + G 2h (Figure 2.c) disappears after further milling for 2h with $AlCl_3$ (Figure 2.d). In both materials (*i.e.* Mg alloy + G 2h + $AlCl_3$ 2h and Mg alloy + G 5h + $AlCl_3$ 2h), Mg crystallites size and particles size reduction was observed after additional milling with $AlCl_3$. Indeed, Mg crystallites size slightly decrease from 28 nm to

23 nm for Mg alloy + G 2h and Mg alloy + G 2h + $AlCl_3$ 2h respectively and from 25 nm to 17 nm for Mg alloy + G 5h and Mg alloy + G 5h + $AlCl_3$ 2h respectively (Table 3). This may be caused by either the presence of $AlCl_3$ which improve ball milling efficiency or by prolonging ball milling time from 2h to 4h or from 5h to 7h. Particle size (*i.e.* d_{90}) reduction from greater than 300 µm to 12 µm for Mg alloy + G 2h and Mg alloy + G 2h + $AlCl_3$ 2h is induced by the presence of $AlCl_3$. In fact, SEM images of the latter material reveal the presence of surface defects caused by ball milling with $AlCl_3$ (Figure 3.f). Both chronologically-added materials have excellent hydrolysis properties despite having slightly different Mg crystallite sizes (23 nm vs. 17 nm, *Cf* Table 3) and particles size (12 µm vs. 8 µm, *Cf* Table 3). We have previously shown that the lesser the milling time the better the hydrogen production performance of the material. Effectively, Mg alloy + G 2h + $AlCl_3$ 2h exhibits better hydrolysis performances than Mg alloy + G 5h + $AlCl_3$ 2h with an almost complete hydrolysis reaction in only 5 minutes.

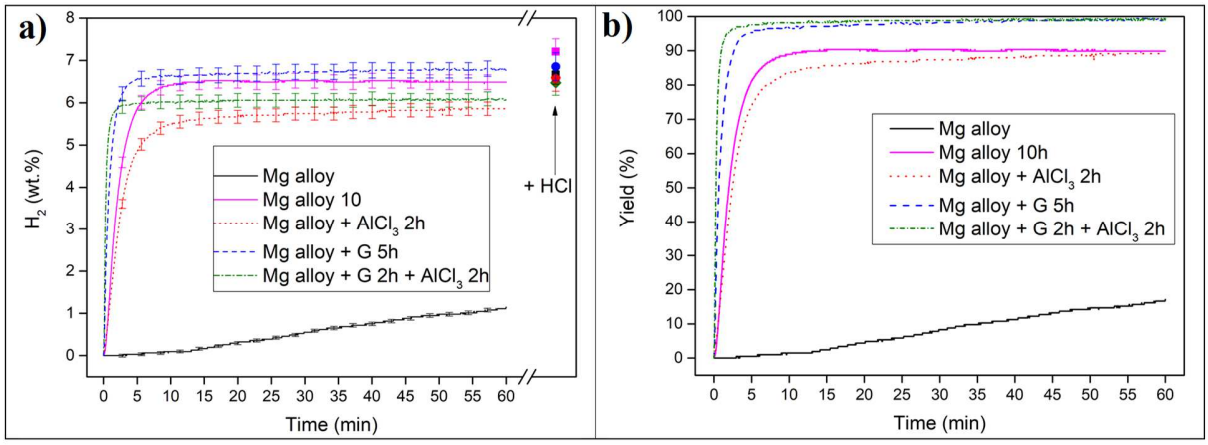

Figure 4: a) Hydrogen released by hydrolysis with Mg alloy, Mg alloymilled for 10h, Mg alloy + $AlCl_3$ 2h, Mg alloy + G 5h and Mg alloy + G 2h + $AlCl_3$ 2h milled under Ar with the P6 and b) the corresponding yield. The amount of hydrogen produced after HCl addition is indicated by the arrow on figure 4.a.

Figure 4 summarizes the influence of each milling strategy performed using the P6 under Ar atmosphere.

Comparing all the materials milled with the P6 under H_2 [2] or under Ar (present study), we note that Mg alloy milled under H_2 showed slightly higher hydrogen generation after 60 minutes but a lower yield due to the formation of less reactive MgH_2. The best strategy with Ar to reach the highest hydrolysis reactivity is to mill Mg alloy only with graphite for 5h or with graphite for 2h followed by milling with $AlCl_3$ for 2h. On the whole, milling under Ar is safer than milling under H_2, and leads to obtaining the most efficient materials in term of hydrolysis performances.

3.3.Effect of ball milling with the Uni-Ball under Ar

In section 3.1, we showed that a process that takes 5 hours with the P6 mill requires roughly 50 hours with the UB mill. We have also shown that: (i) Mg alloy + G provides better hydrolysis performance compared to the single addition of $AlCl_3$ (Section 3.2.2) ; (ii) Mg alloy milled with G for 2h followed by milling with $AlCl_3$ for 2h shows the best hydrolysis performance (total hydrogen generation in 5 minutes) and (iii) milling under Ar gives better hydrolysis performances of Mg alloy compared to milling under H_2. In this context, we investigated the effect of ball milling with graphite and the synergetic effect by the chronological addition of G then $AlCl_3$ under Ar using the UB mill.

As previously demonstrated, milling Mg alloy for 5 hours with graphite is ideal to obtain the best hydrolysis performances (Section 3.2.2). In contrast, the increase in milling time reduces the hydrolysis performance of Mg-based materials [2, 40]. From this basis, we investigated the effect of milling with G for 20h and 50h.

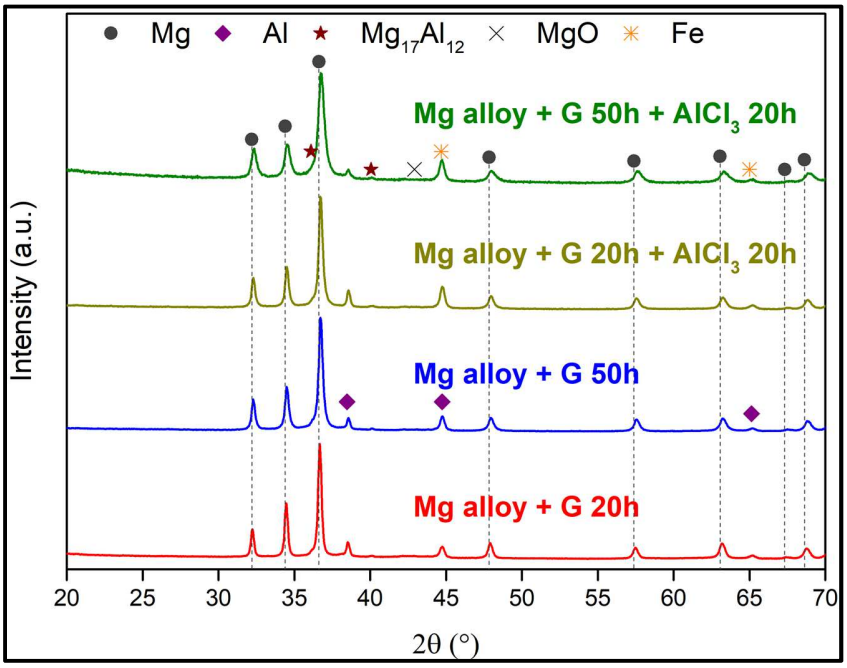

Figure 5: XRD patterns of Mg alloy + G 20h, Mg alloy + G 50h, Mg alloy + G 20h + $AlCl_3$ 20h and Mg alloy + G 50h + $AlCl_3$ 20h milled under Ar with the UB.

XRD patterns of Mg alloy + G 20h and Mg alloy + G 50h (Figure 5.a) shows that Mg (00l) preferential orientation disappears after ball milling. Table 5 indicates that the insertion of Al atoms in Mg matrix increases by prolonging milling time (*i.e.* from 20h to 50h) but it is less pronounced compared to Mg alloy + G milled with the P6 under the same gas. τ_{Mg} and d_{90} for Mg alloy + G decrease by increasing milling time (Table 5 and Figures 6.a and 6.b). Note that τ_{Mg} for Mg alloy + G 20h is slightly higher than Mg alloy + G 2h milled with the P6 under Ar (32 nm vs. 28 nm) while Mg alloy + G 50h and Mg alloy + G 5h exhibit the same crystallites size (25 nm).

Table 5: Al atoms occupancy in Mg matrix (x_{Al}), Mg crystallites size (τ_{Mg}) and particle size d90 of all Mg alloy milled with the UB mill under Ar atmosphere.

Sample	**Rietveld refinement from XRD measurements**		**Particle size d_{90} (µm)**
	x_{Al} in Mg (at.%)	τ_{Mg} (nm)	
Mg alloy	2.2	94	+
Mg alloy + G 20h	0.8	32	17
Mg alloy + G 50h	1.4	25	9
Mg alloy + G 20h + $AlCl_3$ 20h	1.3	26	7
Mg alloy + G 50h + $AlCl_3$ 20h	2.6	15	6

+ the material is not a powder but flakes.

As for the particles size, Mg alloy + G milled with the UB are smaller compared to Mg alloy + G milled with the P6 (Tables 3 and 5). In other words, the insertion of Al into Mg and Mg crystallites size reduction (τ_{Mg}) is weaker and particles size reduction is larger when milling with the UB mill. These findings might be attributed to the fact that the milling with the UB is 10 times longer than the milling with the P6, consequently the number of collisions between the powder and milling balls/chamber wall will be higher, which will further reduce the particles size.

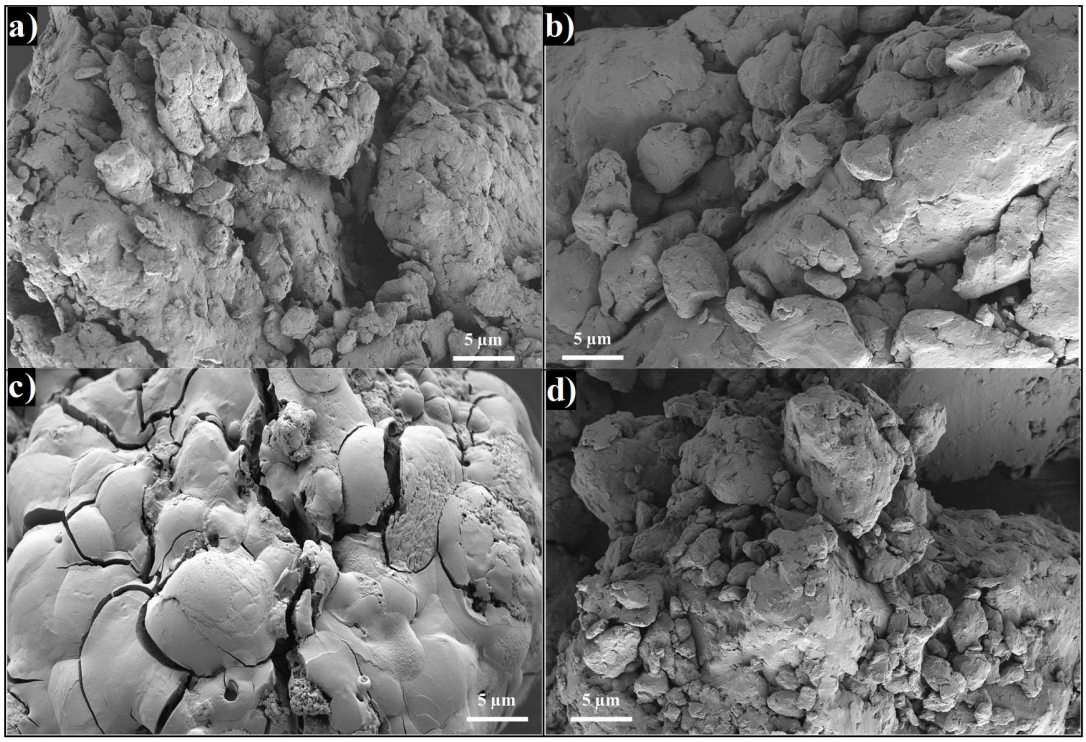

Figure 6: SEM images of a) Mg alloy + G 20h, b) Mg alloy + G 50h, c) Mg alloy + G 20h + $AlCl_3$ 20h and d) Mg alloy + G 50h + $AlCl_3$ 20h milled under Ar with the UB.

Figure 7 shows that the hydrolysis performance of Mg alloy + G 20h and Mg alloy + G 50h are rather similar with an approximate generation of 6.2 wt.% H_2 (corresponding to a yield of 97% of their total capacity) after 5 minutes of reaction (*Cf* Table 6). This is attributed, as mentioned earlier, to particles size reduction and the presence of the protective graphite layer on the surface.

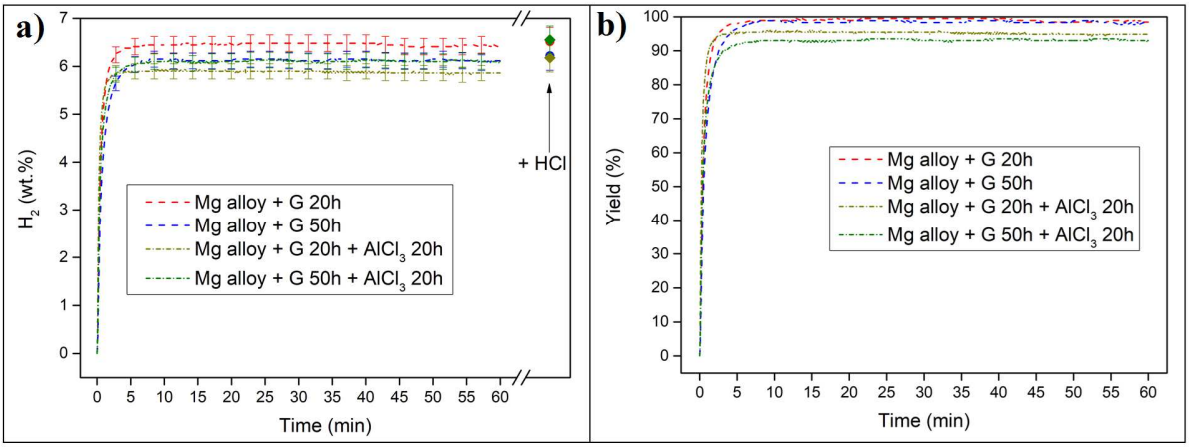

Figure 7: a) Hydrogen released by hydrolysis with Mg alloy + G 20h, Mg alloy + G 50h, Mg alloy + G 20h + $AlCl_3$ 20h and Mg alloy + G 50h + $AlCl_3$ 20h milled under Ar with the UB and b) the corresponding yield. The amount of hydrogen produced after HCl addition is indicated by the arrow on figure 7.a.

We have seen in section 3.2.3 and in a previous work [2] that a further mill of Mg alloy + G 2h and Mg alloy + G 5h with additional milling for 2h with $AlCl_3$ significantly improves the hydrolysis performance. Given the fact that milling should be 10 times longer when using the UB, we milled Mg alloy + G 20h and Mg alloy + G 50h and added an extra 20h milling with $AlCl_3$. Adding $AlCl_3$ increases milling efficiency (*e.g.* x_{Al} increases while τ_{Mg} and d_{90} decrease, *Cf* Table 5). Interestingly, Mg alloy + G 20h + $AlCl_3$ 20h and Mg alloy + G 50h + $AlCl_3$ 20h shows approximately the same Al atoms occupancy and Mg crystallites size as Mg alloy + G 2h + $AlCl_3$ 2h and Mg alloy + G 5h + $AlCl_3$ 2h prepared with the P6, respectively (Tables 3 and 5). On one hand, the presence of $AlCl_3$ during ball milling favors particles size reduction (d_{90} decrease from 17 µm to 7 µm and from 9 µm to 6 µm, *Cf* Table 5) and the formation of surface defects (*i.e.* cracks) as shown in figures 6c and 6d. On the other hand, the beneficial effect of $AlCl_3$ on the hydrolysis performance of Mg alloy milled with graphite is not observable since the latter materials show already excellent performance (Figure 7 and Table 6).

Table 6: Hydrogen production by hydrolysis with Mg alloy milled with the UB mill after 5 minutes and 60 minutes of reaction in 0.6M $MgCl_2$ solution, after 0.5M HCl solution addition considered as being the total hydrogen amount produced) and the calculated yield.

Sample	Mill gas	H_2 generation in 0.6M $MgCl_2$ after 5 minutes		60 minutes		H_2 (wt.%) generation in 0.5M HCl**
		H_2 (wt.%)	Yield (%)*	H_2 (wt.%)	Yield (%)*	
Mg alloy		0.03 ± 0.03	0.5	1.1 ± 0.1	17.2	6.7 ± 0.2
Mg alloy 35h	H_2	3.5 ± 0.1	43.8	6.8 ± 0.2	83.8	8.1 ± 0.3
Mg alloy 50h	H_2	3.5 ± 0.1	42.4	6.3 ± 0.2	75.3	8.3 ± 0.3
Mg alloy 100h	H_2	3.2 ± 0.1	32.6	5.1 ± 0.1	52.2	9.7 ± 0.3
Mg alloy + G 20h	Ar	6.4 ± 0.2	97.9	6.4 ± 0.2	98.4	6.5 ± 0.3
Mg alloy + G 50h	Ar	6.0 ± 0.2	96.6	6.1 ± 0.2	98.3	6.2 ± 0.3
Mg alloy + G 20h + $AlCl_3$ 20h	Ar	5.9 ± 0.2	94.9	5.9 ± 0.2	95.5	6.2 ± 0.3
Mg alloy + G 50h + $AlCl_3$ 20h	Ar	6.0 ± 0.2	92.0	6.1 ± 0.2	93.0	6.6 ± 0.3

* Values are normalized with respect to the total H_2 generated after the addition of 0.5M HCl solution.

** After adding HCl, the hydrolysis reaction is considered complete and the amount of hydrogen produced is considered as the maximum H_2 production.

These results confirm that the equivalence between P6 and UB mills determined in section 3.1 persists when milling under Ar.

4. Conclusions

In conclusion, we investigated the effect of ball milling strategy (*e.g.* milling device, milling gas, additives, etc.) on the hydrolysis performance of Mg alloy waste. The equivalence between a "high-energy" mill (*i.e.* P6) and a "low-energy" mill (*i.e.* UB) was established by comparing Mg hydriding amount and microstructural data after milling the alloy without additives under H_2. A process that takes 5 hours with the P6 mill takes 50 hours with the UB mill. These findings permit the application of equivalent milling strategies for both the P6 and the UB mills.

Milling Mg alloy without additives in the P6 under Ar improves the hydrolysis performances (e.g. Mg alloy milled 10h produces 58% of its total H_2 capacity in 5 minutes). This is attributed to the reduction in particles size (d_{90} going down to 19 µm) which increases the surface area of fresh

reactive Mg. On the other hand, the optimal milling times with $AlCl_3$ or graphite addition are similar (*i.e.* 2h and 5h respectively) to those obtained previously (*i.e.* when Mg alloy was milled under H_2) [2]. The presence of $AlCl_3$ hampers the formation of the passivation film during hydrolysis by decreasing the pH. Graphite addition, by its lubricating effect, delays the reduction of Mg alloy flakes into powder and form a graphite layer which prevent the establishment of the passive layer on the surface. After 5 h of milling, Mg alloy + G 5h generated 95% of its total capacity in 5 minutes and a complete hydrolysis reaction in 60 minutes.

The simultaneous addition of graphite and $AlCl_3$ did not improve the hydrolysis performance and the persistence of the preferential orientation along the c axis for Mg after 10 h of milling indicates that the lubricating effect of graphite is more pronounced in the presence of $AlCl_3$. However, by incorporating both additives sequentially, the best material from the hydrogen production point of view was obtained by milling Mg alloy with G for 2h and then adding $AlCl_3$ and milling for 2 extra hours. This material, Mg alloy + G 2h + $AlCl_3$ 2h reached an almost total hydrolysis (*i.e.* 98%) in 5 minutes. Our results showed that milling under Ar is more efficient than milling under H_2.

In an attempt to scale-up our strategy to an industrial scale, the materials milled with the P6 were compared to Mg alloy milled with the UB (larger than P6 and closer from the existing industrial facilities). Mg alloy milled with graphite for 20h under Ar showed a complete hydrolysis reaction after 5 minutes. However, the effect of $AlCl_3$ was not clearly noticeable due to the already fast H_2 production.

Finally, this study showed that, to modify the reactivity of the alloy with respect to the aqueous solution with an optimal hydrolysis performance, Mg alloy waste should be milled under Ar. On the other hand, the best materials milled with the "high-energy" P6 mill and with the "low-energy" UB mill showed excellent hydrolysis performance indicating that the laboratory-scale milling strategy can be applied on an industrial scale.

Acknowledgements

This work was financially supported by the AZM & Saade Association, the Lebanese University, MINCyT-ECOS-SUD (project number A17A03), CONICET (PIP 0610) and Universidad Nacional de Cuyo (06/C602). Authors also thank Lisea Carbone foundation for financial support and also Fondation Bordeaux Université (Mr Adrien Le Léon and Mrs Iryna Danylyshyna) for valuable help on administrative duty. Bernardo Pentke is acknowledge for his assistance with the scanning electron microscope and Marie-Anne Dourges for the analysis of Mg alloy waste by ICP.

Highlights

1. Milling under Ar is more efficient than milling under H_2.
2. Milling time with the "low-energy" mill is 10 times longer than that with the "high-energy" mill.
3. Total hydrolysis was obtained in 5 minutes for Mg alloy milled with graphite followed by milling with $AlCl_3$ under Ar.
4. Excellent hydrolysis performances are obtained for Mg alloy milled with graphite under Ar.
5. The scale-up of laboratory milling strategy to industrial scale has been established.

Bibliography

1. Sun, Y., et al. Tailoring magnesium based materials for hydrogen storage through synthesis: Current state of the art. Energy Storage Materials 2018;10:168-198. https://doi.org/10.1016/j.ensm.2017.01.010

2. S. Al Bacha, P.S.A., Urretavizcaya, G., M. Zakhour, F.J. Castro, M. Nakhl, J.-L. Bobet. Hydrogen generation from ball milled Mg alloy waste by hydrolysis reaction. Submitted to Energy 2020;

3. Tayeh, T., et al. Production of hydrogen from magnesium hydrides hydrolysis. International Journal of Hydrogen Energy 2014;39:3109-3117. https://doi.org/10.1016/j.ijhydene.2013.12.082

4. Awad, A.S., et al. Effect of carbons (G and CFs), TM (Ni, Fe and Al) and oxides (Nb2O5 and V2O5) on hydrogen generation from ball milled Mg-based hydrolysis reaction for fuel cell. Energy 2016;95:175-186. https://doi.org/10.1016/j.energy.2015.12.004

5. Alasmar, E., et al. Hydrogen generation from Nd-Ni-Mg system by hydrolysis reaction. Journal of Alloys and Compounds 2018;740:52-60. https://doi.org/10.1016/j.jallcom.2017.12.305

6. Fuster, V., G. Urretavizcaya, and F.J. Castro. Characterization of MgH2 formation by low-energy ball-milling of Mg and Mg+C (graphite) mixtures under H2 atmosphere. Journal of Alloys and Compounds 2009;481:673-680. https://doi.org/10.1016/j.jallcom.2009.03.056

7. Al Bacha, S., et al. Hydrogen generation via hydrolysis of ball milled WE43 magnesium waste. International Journal of Hydrogen Energy 2019;44:17515-17524. https://doi.org/10.1016/j.ijhydene.2019.05.123

8. Kuziora, P., et al. Why the ball to powder ratio (BPR) is insufficient for describing the mechanical ball milling process. International Journal of Hydrogen Energy 2014;39:9883-9887. https://doi.org/10.1016/j.ijhydene.2014.03.009

9. Suryanarayana, C. Mechanical alloying and milling. Progress in Materials Science 2001;46:1-184. https://doi.org/10.1016/S0079-6425(99)00010-9

10. Grosjean, M.-H., et al. Effect of ball milling on the corrosion resistance of magnesium in aqueous media. Electrochimica Acta 2004;49:2461-2470. https://doi.org/10.1016/j.electacta.2004.02.001

11. Al Bacha, S., et al. Effect of ball milling in presence of additives (Graphite, $AlCl_3$, $MgCl_2$ and NaCl) on the hydrolysis performances of $Mg_{17}Al_{12}$. International Journal of Hydrogen Energy 2020;45:6102-6109. https://doi.org/10.1016/j.ijhydene.2019.12.162

12. Al Bacha, S., A. Desmedt, and J.L. Bobet. Experimental evidence of H_2 spillover during the corrosion of $Mg_{17}Al_{12}$. Submitted to Energy & Fuels 2020;

13. Grosjean, M.H., M. Zidoune, and L. Roué. Hydrogen production from highly corroding Mg-based materials elaborated by ball milling. Journal of Alloys and Compounds 2005;404-406:712-715. https://doi.org/10.1016/j.jallcom.2004.10.098

14. Sevastyanova, L.G., et al. Hydrogen generation by oxidation of “mechanical alloys” of magnesium with iron and copper in aqueous salt solutions. International Journal of Hydrogen Energy 2017;42:16961-16967. https://doi.org/10.1016/j.ijhydene.2017.05.242

15. Zou, M.-S., et al. Effect of the storage environment on hydrogen production via hydrolysis reaction from activated Mg-based materials. Energy 2014;76:673-678. https://doi.org/10.1016/j.energy.2014.08.065

16. Wang, C., et al. Hydrogen generation by the hydrolysis of magnesium–aluminum–iron material in aqueous solutions. International Journal of Hydrogen Energy 2014;39:10843-10852. https://doi.org/10.1016/j.ijhydene.2014.05.047

17. Buryakovskaya, O.A., M.S. Vlaskin, and S.S. Ryzhkova. Hydrogen production properties of magnesium and magnesium-based materials at low temperatures in reaction with aqueous solutions. Journal of Alloys and Compounds 2019;785:136-145. https://doi.org/10.1016/j.jallcom.2019.01.003

18. Kravchenko, O.V., et al. Formation of hydrogen from oxidation of Mg, Mg alloys and mixture with Ni, Co, Cu and Fe in aqueous salt solutions. International Journal of Hydrogen Energy 2014;39:5522-5527. https://doi.org/10.1016/j.ijhydene.2014.01.181

19. Xiao, F., et al. Hydrogen generation from hydrolysis of activated magnesium/low-melting-point metals alloys. International Journal of Hydrogen Energy 2019;44:1366-1373. https://doi.org/10.1016/j.ijhydene.2018.11.165

20. Grosjean, M.-H. and L. Roué. Hydrolysis of Mg–salt and MgH2–salt mixtures prepared by ball milling for hydrogen production. Journal of Alloys and Compounds 2006;416:296-302. https://doi.org/10.1016/j.jallcom.2005.09.008

21. Zou, M.-S., et al. The preparation of Mg-based hydro-reactive materials and their reactive properties in seawater. International Journal of Hydrogen Energy 2011;36:6478-6483. https://doi.org/10.1016/j.ijhydene.2011.02.108

22. Wang, S., et al. Hydrolysis reaction of ball-milled Mg-metal chlorides composite for hydrogen generation for fuel cells. International Journal of Hydrogen Energy 2012;37:6771-6775. https://doi.org/10.1016/j.ijhydene.2012.01.099

23. Liu, Y., et al. Hydrogen generation from the hydrolysis of Mg powder ball-milled with AlCl3. Energy 2013;53:147-152. https://doi.org/10.1016/j.energy.2013.01.073

24. Kravchenko, O.V., et al. Hydrogen generation from magnesium oxidation by water in presence of halides of transition and non-transition metals. International Journal of Hydrogen Energy 2015;40:12072-12077. https://doi.org/10.1016/j.ijhydene.2015.06.141

25. Sun, Q., et al. A study of hydrogen generation by reaction of an activated Mg–CoCl2 (magnesium–cobalt chloride) composite with pure water for portable applications. Energy 2015;79:310-314. https://doi.org/10.1016/j.energy.2014.11.016

26. Huang, M., et al. Hydrogen production via hydrolysis of Mg-oxide composites. International Journal of Hydrogen Energy 2017;42:22305-22311. https://doi.org/10.1016/j.ijhydene.2016.12.099

27. Huang, M., et al. Enhanced hydrogen generation by hydrolysis of Mg doped with flower-like MoS2 for fuel cell applications. Journal of Power Sources 2017;365:273-281. https://doi.org/10.1016/j.jpowsour.2017.08.097

28. Uan, J.-Y., C.-Y. Cho, and K.-T. Liu. Generation of hydrogen from magnesium alloy scraps catalyzed by platinum-coated titanium net in NaCl aqueous solution. International Journal of Hydrogen Energy 2007;32:2337-2343.

29. Uan, J.-Y., et al. Producing hydrogen in an aqueous NaCl solution by the hydrolysis of metallic couples of low-grade magnesium scrap and noble metal net. International Journal of Hydrogen Energy 2009;34:1677-1687.

30. Uan, J.-Y., et al. Evolution of hydrogen from magnesium alloy scraps in citric acid-added seawater without catalyst. International Journal of Hydrogen Energy 2009;34:6137-6142.

31. Yu, S.-H., J.-Y. Uan, and T.-L. Hsu. Effects of concentrations of NaCl and organic acid on generation of hydrogen from magnesium metal scrap. International Journal of Hydrogen Energy 2012;37:3033-3040.

32. Figen, A.K., B. Coşkuner, and S. Pişkin. Hydrogen generation from waste Mg based material in various saline solutions (NiCl2, CoCl2, CuCl2, FeCl3, MnCl2). International Journal of Hydrogen Energy 2015;40:7483-7489.

33. Figen, A.K. and B.C. Filiz. Hydrogen production by the hydrolysis of milled waste magnesium scraps in nickel chloride solutions and nickel chloride added in Marmara Sea and Aegean Sea Water. International Journal of Hydrogen Energy 2015;40:16169-16177.

34. Pighin, S.A., et al. Nanostructured Mg for hydrogen production by hydrolysis obtained by MgH_2 milling and dehydriding. Journal of Alloys and Compounds 2020 827:154000. https://doi.org/10.1016/j.jallcom.2020.154000

35. TOPAS V4: General Profile and Structure Analysis Software for Powder Diffraction Data, User's Manual, Bruker AXS, Karlsruhe, 2008.

36. Murray, J.L. The Al–Mg (Aluminum−Magnesium) system. Journal of Phase Equilibria 1982;3:60. 10.1007/bf02873413

37. Yamada, K. and C.C. Koch. The influence of mill energy and temperature on the structure of the TiNi intermetallic after mechanical attrition. Journal of Materials Research 1993;8:1317-1326. 10.1557/JMR.1993.1317

38. Moradi, R. and K.M. Groth. Hydrogen storage and delivery: Review of the state of the art technologies and risk and reliability analysis. International Journal of Hydrogen Energy 2019;44:12254-12269. https://doi.org/10.1016/j.ijhydene.2019.03.041

39. Li, S., et al. Influence of chloride salts on hydrogen generation via hydrolysis of MgH2 prepared by hydriding combustion synthesis and mechanical milling. Transactions of Nonferrous Metals Society of China 2017;27:562-568. https://doi.org/10.1016/S1003-6326(17)60062-1

40. Grosjean, M.H., et al. Hydrogen production via hydrolysis reaction from ball-milled Mg-based materials. International Journal of Hydrogen Energy 2006;31:109-119. https://doi.org/10.1016/j.ijhydene.2005.01.001